Hetero-apertured Micro/Nanostructured Ordered Porous Array: Layer-by-Layered Construction and Structure-Induced Sensing Parameter Controllability

Lichao Jia, Weiping Cai,* Hongqiang Wang, Fengqiang Sun, and Yue Li

Key Laboratory of Materials Physics, Anhui Key Laboratory of Nanomaterials and Nanotechnology, Institute of Solid State Physics, Chinese Academy of Sciences, Hefei 230031, Anhui, People's Republic of China

ABSTRACT The double-layer hetero-apertured porous films with hierarchical micro/nanoarchitectures were fabricated on a desired substrate, based on a simple and flexible strategy alternately using the monolayer colloidal crystal with different sizes of colloidal spheres as templates. Such films are of biperiodic ordered structures and can be fully lifted off from the substrate and present a freestanding property. The structures and morphologies of the films can be controlled by combination of the colloidal monolayers with different sphere sizes. The corresponding gas sensing devices were also built. Representatively, the In_2O_3 hierarchically micro/nanostructured porous film-based sensors have shown both higher sensitivity and much faster response to NH_3 atmosphere than the corresponding conventional nanostructured ones. Importantly, the gas-sensing parameters (*i.e.*, response time and the sensitivity) can be well-controlled separately in a large range simply by changing the pore sizes in different layers of the porous film. Further, for the application, a diagram of gas-sensing parameters (t_R—S diagram) was presented, which can not only give a measurement of sensing performances but also well guide design and fabrication of the hierarchically structure-based sensors with desired sensing performances. This work is an important step toward the practical application of the nanostructured porous film sensors.

KEYWORDS: hetero-apertured porous film · hierarchical micro/nanoarchitectures · structurally induced sensing controllability · gas-sensing devices · oxide semiconductors

Metal oxide gas sensors have attracted much attention because of their applications in medical diagnosis, environmental monitoring, personal safety, and national security.[1−4] Their sensing performances depend on the interaction between the testing gas molecules and the adsorbed oxygen molecules on the surface of sensing films. Thus, the structural parameters of the film including pore size, surface area, and film thickness can greatly influence the properties of the sensors.[5−8] Up to now, extensive fundamental and technological efforts have been dedicated to fabricate perfect gas-sensing elements.[9−14] The various nanostructured materials, especially nanoparticles, have been numerously reported for application in gas-sensing devices.[15−18] Compared with those thick compact film-based sensors, nanoparticle-based sensors have achieved superior sensing performance because of their small particle size and high surface area. However, there are still some problems that exist: First, the nanoparticles are usually interconnected and aggregated, which will decrease the specific surface area, and the agglomerate of the particles does not avail the gas diffusion to the interior of the sensing films. Second, these sensing films are usually fabricated by the simple print technique, in which the pore size and homogeneity of the film thickness cannot be precisely controlled, resulting in the uncontrollability of the resulting sensing performance. Therefore, production of the nanostructured films with homogeneous thickness as well as controlled pore size is very important both in scientific interest and in practical application for development of the next generation of nanostructured gas sensors.

Two-dimensional (2D) ordered nanostructure porous films possess high specific surface area and ordered arrangement[19−21] and thus have extensive applications in many areas, such as photonic crystals,[22] catalysis,[23] active substrates for surface-enhanced Raman spectroscopy,[24] data storage media,[25] *etc*. Importantly, these films can be fabricated on any desired substrate (flat or curved surfaces), with the homogeneous and controlled film thickness and the controllable pore sizes, by the solution-dipping, vapor deposition, and electrodeposition based on a template

*Address correspondence to wpcai@issp.ac.cn.

Received for review May 5, 2009 and accepted August 14, 2009.

Published online August 24, 2009.
10.1021/nn900454k CCC: $40.75

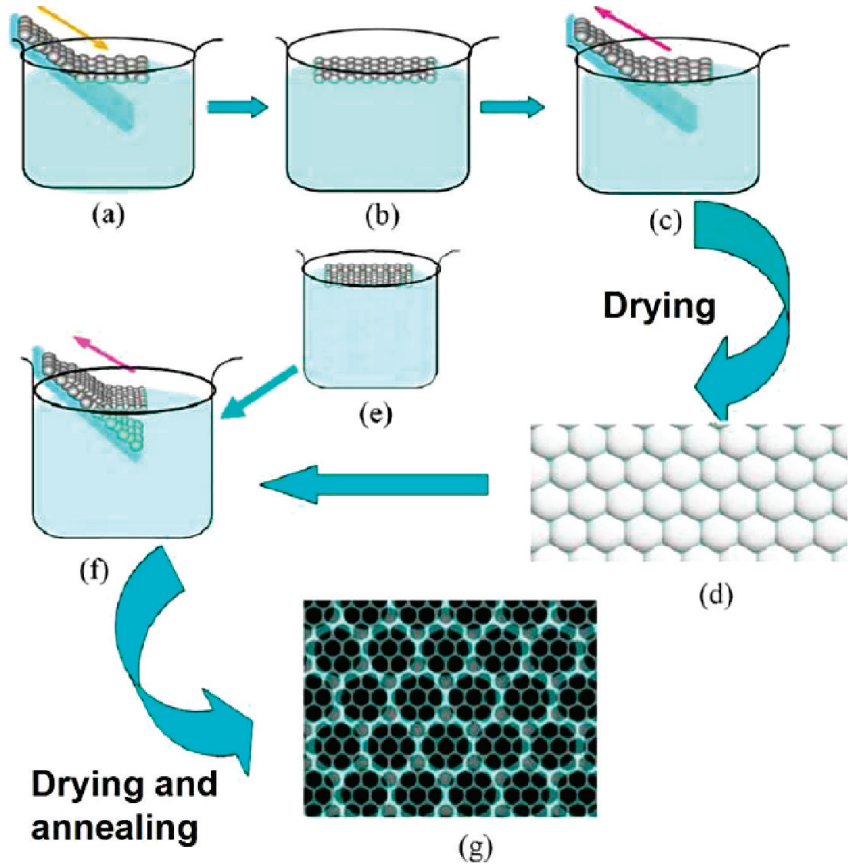

Scheme 1. Outline of the layer-by-layer synthesis strategy for preparing hierarchically micro/nanostructured porous films. (a) Flat glass substrate covered with a colloidal monolayer of 1000 nm PSs is dipped into the precursor solution; (b) the colloidal monolayer floats on the surface of the solution; (c) the monolayer is picked up using a substrate; (d) after drying the substrate with the monolayer in a furnace (120 °C); (e) the colloidal monolayer of smaller PSs (<1000 nm) floats on the surface of the solution [similar to (b)]; (f) using the dried substrate covered with the monolayer (1000 nm PSs) to pick up the colloidal monolayer, with smaller PSs, floating on the solution. (g) The hierarchical micro/nanostructured porous film is formed on the substrate after heat treatment.

strategy of 2D colloidal crystals.[26−29] Thus, such 2D porous films would be good candidates for the new gas-sensing elements,[30−32] and their sensing parameters (sensitivity, response time, *etc.*) can be modulated based on the controllable film structure. However, the two main parameters for such homopore sized porous film-based sensing elements (*i.e.*, the sensitivity and response time) are usually correlated with each other. It means that a large pore size corresponds to a fast response, but low sensitivity, and *vice versa* for a small pore size. The preparation of sensing elements based on such nanostructured porous films with high sensitivity and fast response, as well as separately controllable sensing parameters in a large range, is a great challenge. Solution of this problem will be a big step toward the practical application of the nanostructured porous film-based sensors.

Recently, we have developed a layer-by-layer strategy for fabrication of 2D ordered multilayer oxide porous films with hetero-apertured micro/nanoarchitectures on a desired substrate (flat or curved surfaces) by solution-dipping and alternately using the monolayer colloidal crystal with different sizes of polystyrene spheres (PSs) as templates, as schematically shown in Scheme 1. First, a flat glass substrate covered with a colloidal monolayer of 1000 nm PSs is dipped into the precursor solution. The colloidal monolayer will thus be detached, due to the surface tension of the solution and the difference in the wettability between the glass substrate and the colloidal crystals,[33] and float on the surface of the solution (as shown in Scheme 1a,b). Second, the floating monolayer is picked up using a desired substrate with a flat or curved surface. The colloidal monolayer covers the surface of the substrate and the interstitial space among the PSs, and the space between the colloidal template and the substrate is filled with the solution due to the capillary force. Then, the substrate, with the monolayer and solution, is dried in a furnace (120 °C) (see Scheme 1c,d). Next, we use the dried substrate, covered with the monolayer (1000 nm PSs) and the drying-induced metal hydroxide among their interstitials, as a new substrate to pick up the colloidal monolayer with smaller diameter PSs' floating on the solution (see Scheme 1e,f). Obviously, the precursor solution can wet not only the upper layer with smaller PSs but also the drying-induced metal hydroxide in the bottom layer, making these two layers well-connected after the final treatment. Finally, by drying and annealing the sample to remove the PSs, the hierarchical micro/nanostructured ordered porous film can be obtained on the substrate (Scheme 1g).

Using this strategy, the hierarchical porous films, with any desired layers, can be fabricated on a curved or flat surface. More importantly, the morphology and structure of the porous films can be easily controlled by the solution concentration, the diamater of PS in the templates, *etc*. Also, the corresponding gas-sensing devices can be built by the fabrication of the double-layered porous films, with heteropore sizes, on a ceramic tube, which is usually used for sensor substrates. Here, In_2O_3 is chosen as a model material, which is of high mobility of conduction electrons and chemical/thermal stability,[34,35] to demonstrate the superior sensing performance and parameter controllability of such

hetero-apertured micro/nanostructured porous films. It has been found that these films exhibit both higher sensitivity and faster response to NH_3 at a much lower temperature than the corresponding conventional nanostructured ones. Importantly, the gas-sensing parameters (*i.e.*, response time and the sensitivity) can be modulated in a large range simply by combination of the porous monolayer with different pore sizes. A diagram of gas-sensing parameters is presented, which can give measurement of performance of the sensors. From this diagram, we can easily design and fabricate the multilayer hetero-apertured porous film-based sensing elements with desired sensing performances.

RESULTS AND DISCUSSION

Morphology and Structure. Figure 1a shows the typical morphology of the double-layered hierarchically micro/nanostructured porous film on an ordinary glass slide, which is from the combination of colloidal monolayers with PSs of 1000 and 200 nm in sizes, respectively, for the first and top layers (or 1000/200 nm colloidal monolayers). Apparently, the film is homogeneous. The pores in the film are hexagonally arranged, exhibiting biperiodic ordered structure with periodicities of 1000 and 200 nm, respectively. In addition, this hierarchically structured porous film can be lifted off by blade with integrity, showing a good freestanding property. Figure 1b exhibits the morphology of the back side of the film shown in Figure 1a (deformation of some pores is induced by peeling). We can see that the pores in the first layer are of hollow-spherical shape with truncated tops. The spherical shells or pore walls are very thin (about 30 nm in thickness), and the small holes in the top layer can also be clearly seen from the truncated pores, as more clearly shown in the inset of Figure 1b.

Such a hierarchically structured porous film is significantly different in morphology from the double-layer porous film fabricated by the colloidal monolayers with the same PS diameter, as illustrated in Figure 1c, corresponding to the double-layer porous film from the 200 nm PSs template. It consists of double-layered and closely hexagonally arranged pores with the same size. Each pore in the top layer is situated on the center of three closely packed pores in the first layer. The X-ray diffraction (XRD) indicates that these films are composed of cubic In_2O_3, as shown in Figure 2. The formation of the hierarchically micro/nanostructured porous films is easily understood, which can be attributed to the interstitial geometry of the PS template and solvent evaporation, similar to that of the homopore sized porous films.[33,36] This free-standable and hierarchical porous film is of high surface−volume ratio, controlled pore sizes, and homogeneous film thickness and could be used for smart filters, flowmeters, or for separating tools for biomolecules. Moreover, the as-prepared hierarchically structured porous films are highly expected to be good candidates for new gas-sensing elements, and that is what we are concerned with in this paper.

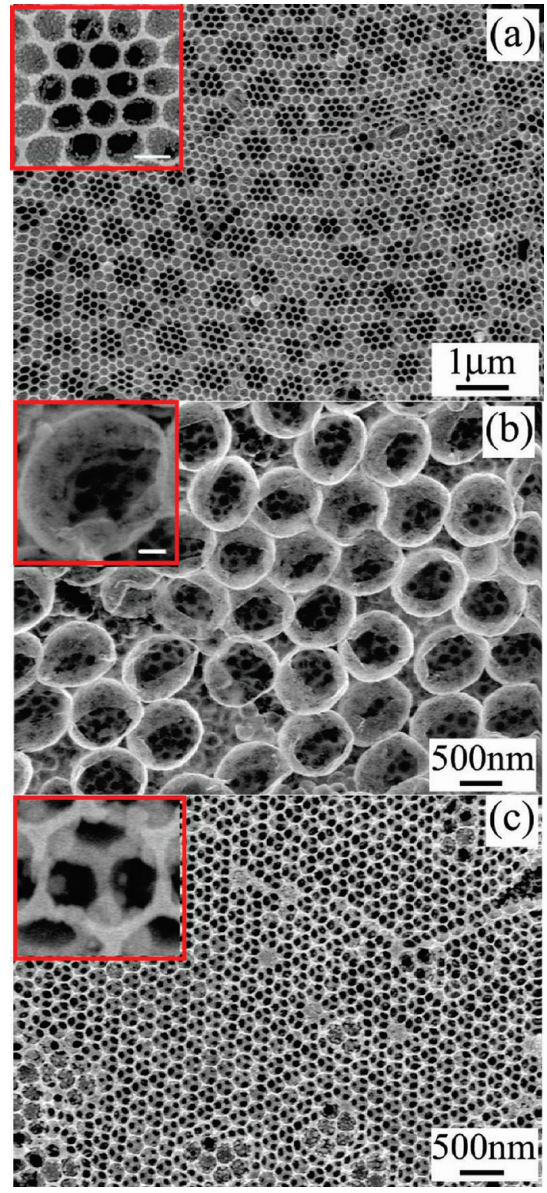

Figure 1. FESEM images of micro/nanostructured porous films on glass substrate. (a) In_2O_3 hierarchical porous structure (1000/200 nm). (b) Back side of the film shown in (a) by peeling. (c) Bilayered homopore sized porous film (200/200 nm). Insets: the local magnification (the scale bars are 200 nm).

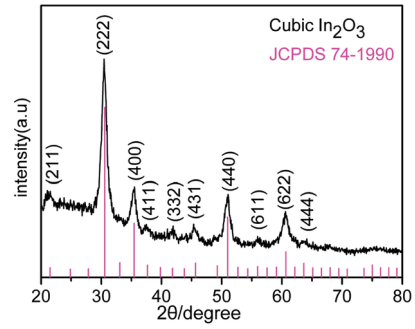

Figure 2. XRD pattern of the film shown in Figure 1a (vertical lines: JCPDS #74-1990, cubic In_2O_3).

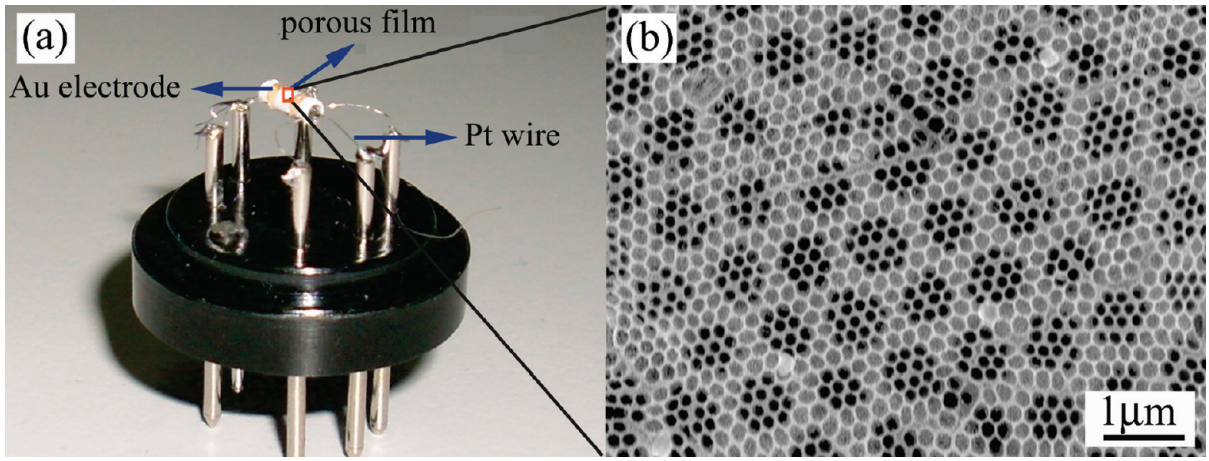

Figure 3. (a) Hierarchically structured porous film (1000/200 nm)-based sensor on a ceramic tube and (b) FESEM image of the film marked in (a).

Gas-Sensing Properties. On the basis of the same method, we can directly fabricate the double-layer hierarchically micro/nanostructured porous film on the surface of a commercial ceramic tube with two preformed gold electrodes at the parts close to its two ends and one Pt wire inside the tube for heating, as illustrated in Figure 3a (the length and outer and inner diameters of the tube are about 5, 2, and 1 mm, respectively). In this way, we can get a series of nanostructured gas sensors with different pore sizes. The morphology of the film on the ceramic tube is representatively illustrated in Figure 3b, which is similar to that shown in Figure 1a.

Gas-Sensing Performance with Both High Sensitivity and Fast Response. The electric response measurements in the NH_3 atmosphere have shown that the gas sensitivity and response time of the sensors are significantly dependent on the structure and morphology of the films. Figure 4 presents the response curves to 500 ppm NH_3 gas at the working temperature of about 60 °C for the samples (or sensors) based on the double-layered micro/nanostructured porous films of 1000/200 (the pore size of the first layer is 1000 nm, while the top layer 200 nm), 200/200, and 1000/1000 nm on the ceramic tubes. Herein, the gas sensitivity (S) is defined as a ratio of two electric resistance values or $S = R_{air}/R_{gas}$, where R_{air} is the resistance value of the sensor in air and R_{gas} is the steady value of the resistance after exposure to the test gas.[6−8] Response time (t_R) is defined as the time required for the resistance to reach 90% of the total variation of resistance after exposure to the test gas. For the sample with the homopore sized porous film of 200/200 nm, the gas sensitivity S and response time t_R are about 20.3 and 102 s, respectively, whereas they are 3.5 and 10 s for the 1000/1000 nm, as shown in Figure 4a,b. Obviously, for the samples with the homopore sized porous structure, the big pore size (1000 nm) corresponds to fast response (10 s) but a very low sensitivity (3.5), while the small pore size (200 nm) leads to the opposite situation or high sensitivity (20.3) but with slow response (102 s). For the hierarchically porous structured sample with the 1000/200 nm film, however, the values of S and t_R are 14.7 and 27 s, respectively (see Figure 4c). Undoubtedly, the double-layered hierarchically structured porous film-based sensor combines the advantages of both big and small sized pores

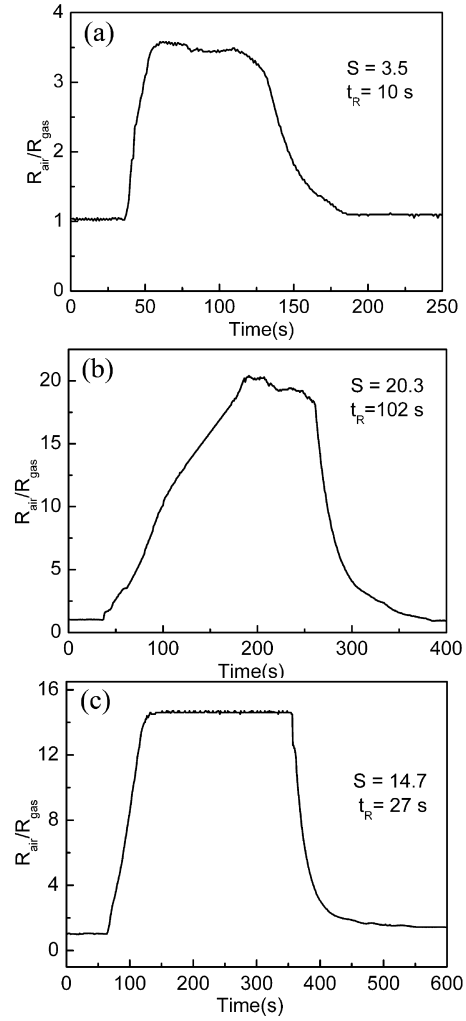

Figure 4. Response curves to 500 ppm NH_3 gas at 60 °C for different double-layer micro/nanostructured porous films. (a) 1000/1000 nm, (b) 200/200 nm, (c) 1000/200 nm.

and has the better sensing performance with both high sensitivity and fast response. Furthermore, it is much more sensitive (9 times higher) than the sensing film of the In_2O_3 nanoparticles, with 30 nm average size, which was fabricated on the ceramic tube with about 1 mm film thickness by a simple printing method, as shown in Figure 5, in addition to the comparable t_R.

Further, the double-layered hierarchically nanostructured porous film exhibits the controllability of t_R and S values just by changing the pore sizes. The flexibility of our synthetic strategy allows for the tunable pore sizes in the hierarchically structured porous films. Figure 6a,b shows the morphology of the double-layered hierarchically micro/nanostructured porous films on the ceramic tubes with 1000/350 and 1000/100 nm, respectively, which is similar to that shown in Figure 1a except the pore sizes in the top layer. Correspondingly, the response curves of 500 ppm NH_3 gas at the same experimental conditions as above are illustrated in Figure 6c,d, respectively, showing a good controllability in sensing performance. The controllability of the hierarchical porous structure is highly expected to modulate the gas-sensing parameters, such as S and t_R, in a large range, according to practical application.

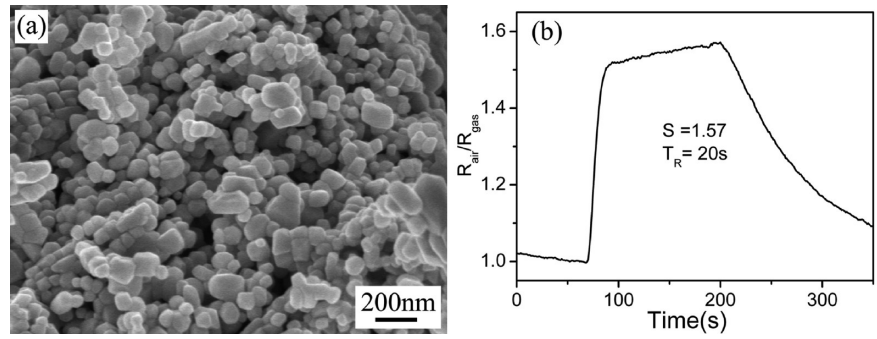

Figure 5. FESEM image (a) and response curve to 500 ppm NH_3 at 60 °C (b) for the In_2O_3 nanoparticle film, which was fabricated on the ceramic tube with about 1 mm film thickness by a simple printing method.

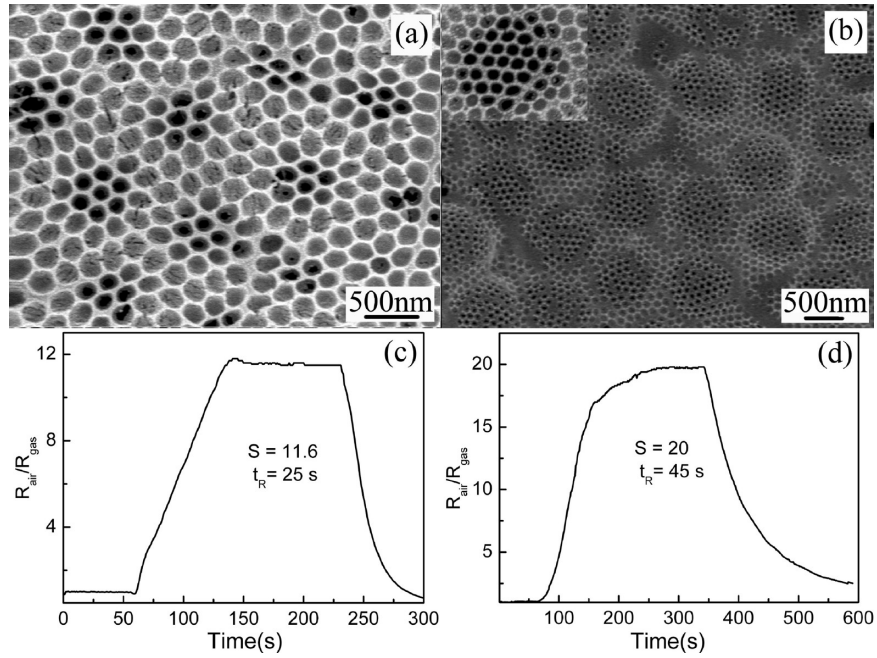

Figure 6. FESEM images of hierarchical micro/nanostructures with different pore size combinations: (a) 1000/350 nm and (b) 1000/100 nm; (c) and (d) response curves of the films shown in (a) and (b) in 500 ppm NH_3, respectively.

The values of S and t_R for all of the samples in this study (for 500 ppm NH_3 test gas) are shown in Figure 7 (a diagram of t_R *versus* S). It can be clearly seen that S value increases mainly with the reduction of the pore size in the top layer when the pore size of the first layer is fixed at 1000 nm (see dashed line in Figure 7). On the contrary, the t_R value mainly depends on the pore size of the first layer (see points c and d in Figure 7). It means that we can control the S value mainly by the pore size of the top layer and the t_R value simply by that of the first layer. We can thus, from such a t_R-S diagram, easily design and fabricate the structure of double-layered porous films with desired sensing parameter according to practical requirements. As an example, if we need a sensor with the sensing parameters (S, t_R) located at point e (the black mark in Figure 7), obviously, the pore size of the top layer should be between 1000 and 350 nm (or between points a and b on the x axis), and that of the first layer should be be-

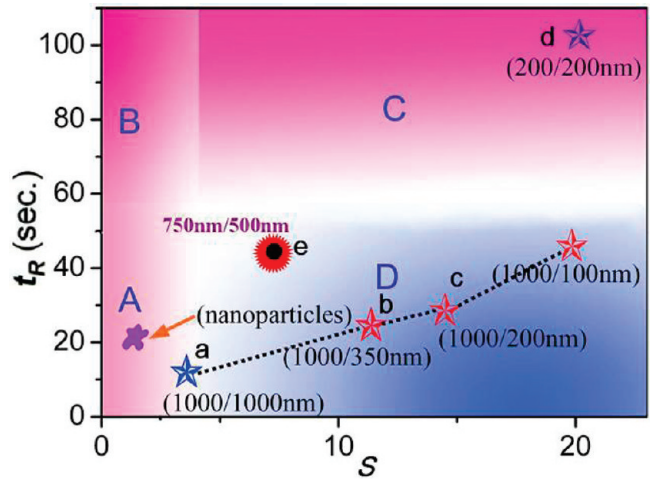

Figure 7. Diagram of the sensing parameters t_R *versus* S for In_2O_3 films with different porous structures in 500 ppm NH_3 atmosphere at 60 °C (see text for details). A−D correspond to the different zones in the diagram.

tween 1000 and 200 nm (or between points a and d but close to point a on the *y* axis), which has been confirmed by further experiment. Position e (the red mark in Figure 7) corresponds to the result of the double-layered hierarchically micro/nanostructured porous film sensor from 750/500 nm.

Furthermore, the t_R-S diagram in Figure 7 can, in principle, give a measurement of the sensing performance of a sensor. Different positions in the diagram correspond to different sensing performances. Obviously, the *S* value is too low in regions A and B, and the response is too slow in regions B and C (see Figure 7), indicating that the sensors with sensing parameters in these regions are unfavorable in practical use.[5,7] The parameters in region D correspond to both fast response and high sensitivity and hence are of practical application.

We also examined the gas-sensing performances of all the films for the other concentrations (from 20 to 2000 ppm) of the NH_3 test gas, as shown in Figure 8a. Obviously, the sensitivity of all the films shows similar increase with the rising concentration of NH_3 gas. Further, evolution of the sensing parameters with pore size is similar to that in Figure 7, as illustrated in Figure 8b. It should be mentioned that the on and off responses in this study were repeated for more than 50 cycles without observing significant changes in the *S* and t_R values, indicating the good reproducibility of the sensing performance. Also, the sensing performances keep almost the same after a long-time preservation in air (about 6 months) for our samples, showing the good sensing stability, as illustrated in Figure S1 in the Supporting Information. It is expected that combination of the monolayer porous structure with different pore sizes into the multilayer (more than two layers) hierarchically micro/nanostructured porous films would lead to the controllability of *S* and t_R values of sensors in a large range and meet various practical requirements.

Structurally Induced Controllability of Gas-Sensing Property. For In_2O_3-based sensing elements, the change in resistance is caused by the redox reaction on the surface of the In_2O_3 film in a gas atmosphere. When the film is exposed to air, oxygen in air is chemisorbed as O^{2-} ions on its surface, and some electrons in the film are localized in the film surface, leading to an increase of the resistance.[35,37] When exposed to a reducing gas, NH_3, for instance, the redox reaction occurs at a certain temperature between the reducing gas and the adsorbed oxygen molecules, and the amount of the adsorbed oxygen will thus be decreased, inducing release of the surface-trapped electrons back to the In_2O_3 film and hence significant reduction of resistance. Thus, many factors can influence the sensing performance, such as the mobility of conduction electrons and the chemical/thermal stability of metal oxide, the surface area, the pore size, and crystallite/grain size of the films, *etc.* For a given film, the gas-sensing performance should mainly depend on crystallite/grain and pore sizes of the film.

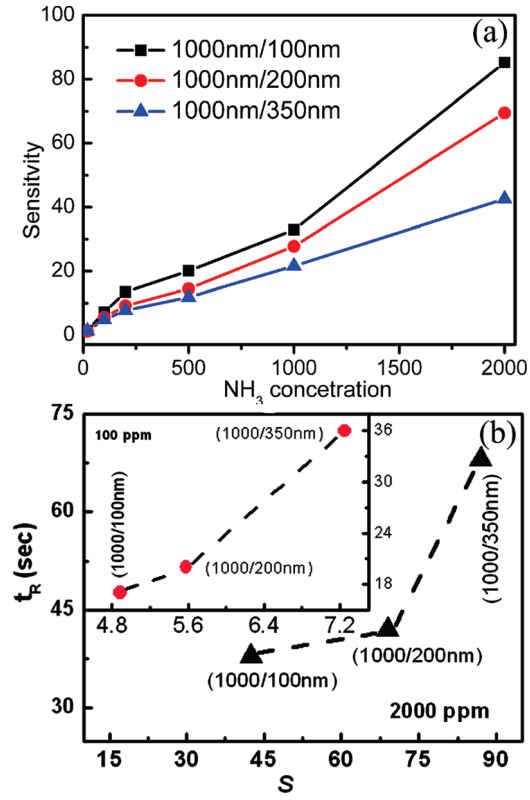

Figure 8. Sensitivity as a function of NH_3 concentration (a) and diagram of t_R *versus* *S* in 2000 and 100 ppm (inset) NH_3 (b) at 60 °C for the different double-layer hierarchically structured porous In_2O_3 films (1000/100, 1000/200, 1000/350 nm).

In this study, the fabrication conditions (precursor solution concentration, and drying and subsequent annealing treatment, *etc.*) are the same for all of the samples with different pore sizes. It means that the crystallite/grain sizes for all of the samples should be similar (about 12 nm), which has been confirmed by XRD results (see Figure 2 and Figure S2 in Supporting Information). So, the structure-induced controllability of the gas-sensing property in this study is mainly attributed to different pore sizes. Obviously, the higher surface area (or smaller pore size) exposed to environmental atmosphere corresponds to the higher *S* value.[6] Meanwhile, in our case, the smaller pore size in the top layer corresponds to the smaller pore area at the film surface, which will thus decrease the transportation rate of the gas molecules and diffusion along the pore wall within the porous film when exposed to the test gas atmosphere and increase the response time t_R. The results in this study are thus easily understood. When decreasing the pore size in the top layer (keeping that of the first layer), the *S* value will rise due to increase of the specific surface area, but the response rate slows down because of the difficult small pore-induced transportation of the test gas. Additionally, the peculiar hierarchical micro/nanostructure will lead to significantly more dangling bonds or higher surface activity for the reaction of the reducing gas with adsorbed oxygen molecules than

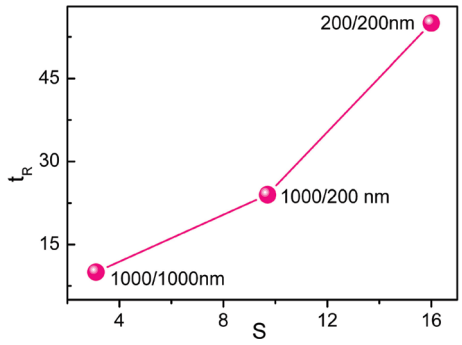

Figure 9. Diagram of the sensing parameters t_R *versus* S for Fe_2O_3 micro/nanostructured films with different double-layer porous structures in 500 ppm NH_3 atmosphere at 60 °C.

for the bulk structure[13,38] and thus remarkably decrease the reaction temperature. In this study, our working temperature is only 60 °C, much lower than that (about 300 °C) of the other In_2O_3 sensors,[16,35] which is very important for the practical application, especially for detection of some flammable gas.

All in all, by combining the monolayer porous structure with different pore sizes into multilayered hierarchically micro/nanostructured porous films, we can modulate both S and t_R values separately in a large range and obtain the sensors with desired sensing performance, or both high sensitivity and fast response, to meet practical requirements. Such sensors are superior to those of the nanoparticle-based ones and can overcome the shortages of the homopore sized porous films mentioned in the introduction section and can improve the S and t_R values to desirable values.

Universality of the Strategy. Further, the strategy presented in this paper can also be used for some other oxide semiconductor hetero-apertured porous films with hierarchical micro/nanoarchitectures. We have successfully fabricated such porous films as SnO_2, Fe_2O_3, TiO_2, ZnO, CuO, *etc.* and obtained structurally induced tunable sensing parameters and better sensing performances than the conventional nanostructured ones. Representatively, Figure S3 in the Supporting Information gives the results of Fe_2O_3, which is a widely used material in the gas-sensor industry. Correspondingly, the hetero-apertured porous Fe_2O_3 film with hierarchical micro/nanostructure shows both high sensitivity and fast response and is better than that of homopore sized porous film, as shown in Figure 9 (data from Figure S3 in Supporting Information). Further, we can get some doped oxides by adding different dopant ions into the precursor solution, which can further improve the sensing performance. Besides, it is highly expected that the hetero-multilayer hierarchical micro/nanostructured porous films could be fabricated by alternately using several different precursor solutions. Such films could be of high performance for detection of multiple gases. Also, the film surface can be decorated with some specific organic and bio-organic receptors in order to get higher selectivity.

CONCLUSIONS

In summary, the double-layered hetero-apertured porous films with hierarchical micro/nanoarchitectures and controlled pore size were fabricated on the desired substrates, based on a simple and flexible layer-by-layer strategy using the monolayer colloidal crystal with different sizes of colloidal spheres as templates. Such films are of biperiodic ordered structures and can be wholly lifted off from the substrate and present a freestanding property. The hierarchically micro/nanostructured porous film-based gas sensors on the ceramic tube show both high sensitivity and fast response to NH_3 gas and are superior to traditional ones. Importantly, such a sensor can overcome the shortages of the homopore sized porous film-based sensors and improve the sensitivity and the response time to the desirable values. The S and t_R can be separately modulated in a large range by combination of the monolayer porous films with different pore sizes. Moreover, the peculiar hierarchical micro/nanostructure can remarkably decrease the reaction temperature owing to the increasing dangling bonds or the surface activity for the reaction of the reducing gas with adsorbed oxygen molecules. A diagram of gas-sensing parameters t_R *versus* S was presented, which can give measurement of the sensing performance of sensors. We can thus design and fabricate the hierarchically micro/nanostructured sensors with desired sensing performance. This work could be an important step toward the practical application of the nanostructured porous film-based sensors and could provide the realization in the near future of new types of practical micro/nanostructured gas-sensing devices.

EXPERIMENTAL DETAILS

Fabrication of Hetero-apertured Porous Films and Its Sensing Devices. Ordinary glass slides were washed with acetone, ethanol, and distilled water in an ultrasonic bath and then in turn cleaned in 98% H_2SO_4/H_2O_2 (3:1 in volume), $H_2O/NH_3 \cdot H_2O/H_2O_2$ (5:1:1 in volume), and distilled water, respectively. Suspensions of monodispersed PSs (2.5 wt % in water, surfactant-free) were obtained from Alfa Aesar Corporation. Large-area (*ca.* 1 cm^2) ordered PS colloidal monolayers were synthesized by the spin-coating method on a custom-built spin coater. A 0.1 M $In(NO_3)_3$ aqueous solution was used as precursor solution. The glass slide covered with the colloidal monolayer of 1000 nm PSs was gradually immersed into the precursor solution at a certain angle, as shown in Scheme 1a. The colloidal monolayer was then lifted off from the glass substrate and floated on the surface of the precursor solution. Next, the monolayer was picked up with a desired substrate (ceramic tube with curved surface or some other substrates with flat surface) and

heated at 120 °C for 0.5 h in an oven. Subsequently, we used the dried substrate covered with the monolayer to pick up another colloidal monolayer with different PS diameters (350, 200, or 100 nm, and so on) floating on the solution and then dried it at 120 °C for 0.5 h. Finally, the temperature was increased to 400 °C at a rate of 3 °C min^{-1} and was kept at 400 °C for 1 h to burn the PSs away, leaving a hierarchically structured porous film with double layers on the substrate and forming In_2O_3 due to decomposition of $In(NO_3)_3$. Similarly, a gas sensor can be built if the ceramic tube with the preformed gold electrodes at the parts close to its two ends is used as substrate.

Characterization. The morphologies of all the samples were examined on a field-emission scanning electron microscope (FESEM, Sirion 200). Phase analysis of the films was carried out on a Philips X'Pert powder X-ray diffractometer using Cu Kα (0.15419 nm) radiation.

Gas-Sensing Measurements. Gas-sensing experiments were performed in a static system in a custom-built experiment setup (WS-30A) at a low working temperature (about 60 °C). It should be mentioned that there are two small mixing fans mounted in the sample chamber to mix the test gases sufficiently in very short time. All of the measurements were carried out at a relative humidity of 50%, and NH_3 was used as test gas. The Pt wire heater inside the ceramic tube is used to control the temperature of the film.

Acknowledgment. This work is financially supported by Natural Science Foundation of China (Grant Nos. 50831005 and 10874184), the Major State research program of China "Fundamental Investigation on Micro-Nano Sensors and Systems based on BNI Fusion" (Grant No. 2006CB300402), the Knowledge Innovation Program of the Chinese Academy of Sciences (Grant No. KJCX2-SW-W31), and the Anhui Natural Science Foundation (No. 090414188).

Supporting Information Available: Sensing curves, XRD patterns, and SEM images of the ordered porous arrays. This material is available free of charge *via* the Internet at http://pubs.acs.org.

REFERENCES AND NOTES

1. Kohl, D. Function and Applications of Gas Sensors. *J. Phys. D* **2001**, *34*, 125–149.
2. Moos, R.; Sahner, K.; Fleischer, M.; Guth, U.; Barsan, N.; Weimar, U. Solid State Gas Sensor Research in Germany—A Status Report. *Sensors* **2009**, *9*, 4323–4365.
3. Yamazoe, N. Toward Innovations of Gas Sensor Technology. *Sens. Actuators, B* **2005**, *108*, 2–14.
4. Oberg, P. A.; Togawa, T.; Spelman, F. A. Sensors in Medicine and Health Care. In *Sensors Application*; Hesse, J., Gardner, J., Göpel, W., Eds.; Wiley-VCH: Weinheim, Germany, 2004; pp 360−380.
5. Michael, T. Porous Metal Oxides as Gas Sensors. *Chem.—Eur. J.* **2007**, *13*, 8376–8388.
6. Yamazoe, N.; Sakai, G.; Shimanoe, K. Oxide Semiconductor Gas Sensors. *Catal. Surveys Asia* **2003**, *7*, 63–75.
7. Alexander, G.; Ralf, R. *In Situ* and Operando Spectroscopy for Assessing Mechanisms of Gas Sensing. *Angew. Chem., Int. Ed.* **2007**, *46*, 3826–3848.
8. Franke, M. E.; Koplin, T. J.; Simon, U. Metal and Metal Oxide Nanoparticles in Chemiresistors: Does the Nanoscale Matter. *Small* **2006**, *2*, 36–50.
9. Qin, K.; Lao, C. S.; Wang, Z. L.; Xie, Z. X.; Zheng, L. S. High-Sensitivity Humidity Sensor Based on a Single SnO_2 Nanowire. *J. Am. Chem. Soc.* **2007**, *129*, 6070–6071.
10. Kong, J.; Franklin, N. R.; Zhou, C. W.; Chapline, M. G.; Peng, S.; Cho, K.; Dai, H. J. Nanotube Molecular Wires as Chemical Sensors. *Science* **2000**, *287*, 622–625.
11. Hagleitner, C.; Hierlemann, A.; Lange, D.; Kumme, A.; Kerness, N.; Brand, O.; Baltes, H. Single-Chip Gas Sensor Microsystem. *Nature* **2001**, *414*, 293–296.
12. Lee, C. Y.; Strano, M. S. Amine Basicity (pK_b) Controls the Analyte Binding Energy on Single Walled Carbon Nanotube Electronic Sensor Arrays. *J. Am. Chem. Soc.* **2008**, *130*, 1766–1773.
13. Du, N.; Zhang, H.; Chen, B.; Ma, X.; Liu, Z.; Wu, J.; Yang, D. Porous Indium Oxide Nanotubes: Layer-by-Layer Assembly on Carbon-Nanotube Templates and Application Gas Sensors. *Adv. Mater.* **2007**, *19*, 1641–1645.
14. Wang, Y. D.; Djerdj, I.; Antonietti, M.; Smarsly, B. Polymer-Assisted Generation of Antimony Doped SnO_2 Nanoparticles with High Crystallinity for Application in Gas Sensors. *Small* **2008**, *4*, 1656–1660.
15. Buso, D.; Post, M.; Cantalini, C.; Mulvaney, P.; Martucci, A. Gold Nanoparticle-Doped TiO_2 Semiconductor Thin Films: Gas Sensing Properties. *Adv. Funct. Mater.* **2008**, *18*, 3843–3849.
16. Wang, H. Q.; Li, G. H.; Jia, L. C.; Wang, G. Z.; Tang, C. J. Controllable Preferential-Etching Synthesis and Photocatalytic Activity of Porous ZnO Nanotubes. *J. Phys. Chem. C* **2008**, *112*, 11738–11743.
17. Polleux, J.; Gurlo, A.; Barsan, N.; Weimar, U.; Antonietti, M.; Niederberger, M. Template-Free Synthesis and Assembly of Single-Crystalline Tungsten Oxide Nanowires and Their Gas-Sensing Properties. *Angew. Chem., Int. Ed.* **2006**, *45*, 261–265.
18. Waitz, T.; Wagner, T.; Sauerwald, T.; Kohl, C. D.; Tiemann, M. Ordered Mesoporous In_2O_3: Synthesis by Structure Replication and Application as a Methane Gas Sensor. *Adv. Funct. Mater.* **2009**, *19*, 653–661.
19. Wang, J. J.; Li, Q.; Knoll, W.; Jonas, U. Preparation of Multilayered Trimodal Colloid Crystals and Binary Inverse Opals. *J. Am. Chem. Soc.* **2006**, *128*, 15606–15607.
20. Zhang, G.; Wang, D. Y.; Mohwald, H. Ordered Binary Arrays of Au Nanoparticles Derived from Colloidal Lithography. *Nano Lett.* **2007**, *7*, 127–132.
21. Li, Y.; Lee, E. J.; Cai, W. P.; Kim, K. Y.; Cho, S. O. Unconventional Method for Morphology-Controlled Carbonaceous NanoarraysBased on Electron Irradiation of a Polystyrene Colloidal Monolayer. *ACS Nano* **2008**, *2*, 1108–1112.
22. Duan, G. T.; Cai, W. P.; Luo, Y. Y.; Sun, F. Q. A Hierarchically Structured $Ni(OH)_2$ Monolayer Hollow-Sphere Array and Its Tunable Optical Properties over a Large Region. *Adv. Funct. Mater.* **2007**, *17*, 644–650.
23. Ibañez, F. J.; Zamborini, F. P. Reactivity of Hydrogen with Solid-State Films of Alkylamine- and Tetraoctylammonium Bromide-Stabilized Pd, Pd Ag, and Pd Au Nanoparticles for Sensing and Catalysis Applications. *J. Am. Chem. Soc.* **2008**, *130*, 622–633.
24. Duan, G. T.; Cai, W. P.; Luo, Y. Y.; Li, Y.; Lei, Y. Hierarchical Surface Rough Ordered Au Particle Arrays and Their Surface Enhanced Raman Scattering. *Appl. Phys. Lett.* **2006**, *89*, 181918-1–181918-3.
25. Tilley, R. D.; Saito, S. Preparation of Large Scale Monolayers of Gold Nanoparticles on Modified Silicon Substrates Using a Controlled Pulling Method. *Langmuir* **2003**, *19*, 5115–5120.
26. Zhang, G.; Wang, D. Y.; MÖhwald, H. Patterning Microsphere Surfaces by Templating Colloidal Crystals. *Nano Lett.* **2005**, *5*, 143–146.
27. Li, Y.; Cai, W. P.; Duan, G. T.; Li, C. C.; Sun, F. Q.; Zeng, H. B. Morphology-Controlled 2D Ordered Arrays by Heating-Induced Deformation of 2D Colloidal Monolayer. *J. Mater. Chem.* **2006**, *16*, 609–612.
28. Li, Y.; Cai, W. P.; Duan, G. T. Ordered Micro/Nanostructured Arrays Based on the Monolayer Colloidal Crystal. *Chem. Mater.* **2008**, *20*, 615–624.
29. Xie, R. G.; Liu, X. Y. Controllable Epitaxial Crystallization and Reversible Oriented Patterning of Two Dimensional Colloidal Crystals. *J. Am. Chem. Soc.* **2009**, *131*, 4976–4982.
30. Sun, F. Q.; Cai, W. P.; Li, Y.; Jia, L. C.; Lu, F. Direct Growth of Mono- and Multilayer Nanostructured Porous Films on Curved Surfaces and Their Application as Gas Sensors. *Adv. Mater.* **2005**, *17*, 2872–2881.
31. Scott, R.W. J.; Yang, S. M.; Chabanis, G.; Coombs, N.; Williams, D. E.; Ozin, G. A. Tin Dioxide Opals and Inverted Opals: Near-Ideal Microstructures for Gas Sensors. *Adv. Mater.* **2001**, *13*, 1468–1472.

32. Scott, R. W. J.; Yang, S. M.; Coombs, N.; Ozin, G. A.; Williams, D. E. Engineered Sensitivity of Structured Tin Dioxide Chemical Sensors: Opaline Architectures with Controlled Necking. *Adv. Funct. Mater.* **2003**, *13*, 225–231.
33. Sun, F. Q.; Cai, W. P.; Li, Y.; Cao, B. Q.; Lei, Y.; Zhang, L. D. Morphology-Controlled Growth of Large-Area Two-Dimensional Ordered Pore Arrays. *Adv. Funct. Mater.* **2004**, *14*, 283–288.
34. Li, C.; Zhang, D.; Liu, X.; Han, S.; Tang, T.; Han, J.; Zhou, C. In_2O_3 Nanowires as Chemical Sensors. *Appl. Phys. Lett.* **2003**, *82*, 1613–1615.
35. Soulantica, K.; Erades, L.; Sauvan, M.; Senocq, F.; Maisonnat, A.; Chaudret, B. Synthesis of Indium and Indium Oxide Nanoparticles from Indium Cyclopentadienyl Precursor and Their Application for Gas Sensing. *Adv. Funct. Mater.* **2003**, *13*, 553–557.
36. Sun, F. Q.; Yu, J. C. Photochemical Preparation of Two-Dimensional Gold Spherical Pore and Hollow Sphere Arrays on a Solution Surface. *Angew. Chem., Int. Ed.* **2006**, *45*, 1–6.
37. Korotcenkov, G.; Cerneavschi, A.; Brinzari, V.; Vasiliev, A.; Ivanov, M.; Cornet, A.; Morante, J.; Cabot, A.; Arbiol, J. In_2O_3 Films Deposited by Spray Pyrolysis as a Material for Ozone Gas Sensors. *Sens. Actuators, B* **2004**, *99*, 297–303.
38. Liu, Z. F.; Yamazaki, T.; Shen, Y.; Kikuta, T.; Nakatani, N.; Kawabata, T. Room Temperature Gas Sensing of *p*-Type TeO_2 Nanowires. *Appl. Phys. Lett.* **2007**, *90*, 173119-1–173119-3.